3-1-2012

Wallpaper Maps

M. Douglas McIlroy
Dartmouth College, douglas.mcilroy@dartmouth.edu

Wallpaper maps

M. Douglas McIlroy

Dartmouth College, Hanover, NH

March, 2012
Revision 1, March 2021

Substantive changes in this revised version:

- Correct all entries in the last line of Table 5.
- Include a brief addendum about the use of wallpaper maps.

Other changes:

- Simplify the lead-in to Corollary 2.
- Simplify Figure 6.
- Fix four minor typos.
- Renumber references (automatic change).

The original version, published as Dartmouth Computer Science Technical Report TR2012-712, is now available at https://digitalcommons.dartmouth.edu/cs_tr/353/ under "Additional Files". An abbreviated version appeared in a festschrift for Brian Randell.[1]

Wallpaper maps

M. Douglas McIlroy

Dartmouth College, Hanover, NH, USA

ABSTRACT

A wallpaper map is a conformal projection of a spherical earth onto regular polygons with which the plane can be tiled continuously. A complete set of distinct wallpaper maps that satisfy certain natural symmetry conditions is derived and illustrated. Though all of the projections have been published before, some generalize to one-parameter families in which the sphere is pre-transformed by a conformal automorphism.

Within a decade of Schwarz's publication of a formula for conformally mapping a circle onto a regular polygon,[2] the noted American philosopher C. S. Peirce used it to calculate a conformal map of the world in a square (Figure 1), with which the plane can be tiled.[3] The projection (more precisely, its inverse) is doubly periodic, and necessarily possesses isolated branch points,[4] each of which is surrounded by multiple copies of a mapped neighborhood. Other doubly periodic projections were published sporadically, especially by O. S. Adams, until almost a century later L. P. Lee collected them and other polygonal maps in a summary monograph.[5] No more have appeared since. This paper explains why, and in so doing gives a uniform account of this family of projections.

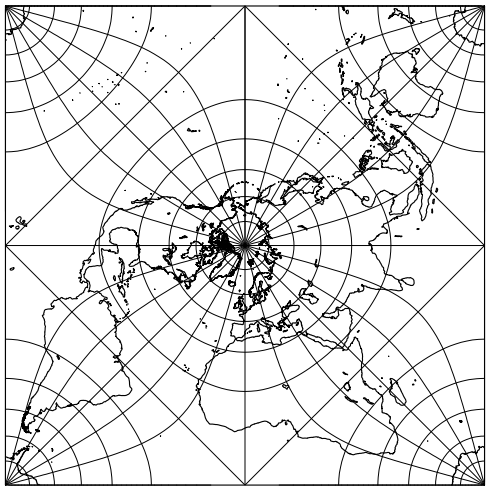

Figure 1. Peirce's projection. A dissected square southern hemisphere is arranged around a square northern hemisphere.

Preliminaries

For our purposes, a *tiling* is a covering of a surface by congruent, non-overlapping regular polygons, or *tiles,* fitted edge-to-edge and vertex-to-vertex. A *tiling projection* is a (one-to-many) conformal map from a tiling of the sphere to a tiling of the plane. Restricted to a single spherical tile and one of its planar image tiles, the map must

(a) be conformal and bijective throughout the interior,
(b) continue across each edge into an adjacent tile, conformally except at isolated singularities,
(c) preserve the symmetry group of each spherical tile, and
(d) be the same in all tiles.

To state requirement (c) more precisely, let G and G' be the (dihedral) symmetry groups of a spherical polygon, X, and one of its planar images, X', respectively; and let $f: X \to X'$ be the mapping function. Then for each $g \in G$ there must exist $g' \in G'$ such that for every point $x \in X$

$$f(g(x)) = g'(f(x)) \tag{1}$$

Requirement (d) says that tile-to-tile symmetries on the sphere and the plane commute with mapping from sphere to plane. If f acts on spherical tiles X and Y to produce images in planar tiles X' and Y' respectively, and g is a symmetry operation on the sphere that takes tile X to Y, then there exists a symmetry operation, g' on the plane that takes X' to Y' such that (1) holds for all points x in X.

The p lines of reflective symmetry in a spherical p-gon must map onto lines of reflective symmetry in the plane. In particular a vertex or the midedge of an edge (hereafter called simply a *midedge*) of a spherical tile must map to a vertex or midedge (not necessarily respectively) in the plane. Also, if $p > 1$, the center of a spherical tile must map to the center of a planar tile.

Call the vertices and midedges collectively *fixable points* and number the fixable points of a spherical p-gon $0, 1, \cdots, 2p-1$ in order around the boundary, so that vertices have even numbers and midedges odd. The fixable points of the corresponding p'-gon image may be numbered similarly, with directions of increase being consistent under the map. A fixable point numbered x on a spherical tile maps to a fixable point numbered $(kx + c) \bmod p'$ on the planar image, where integer c represents a rotation and $k = p'/p$ is a positive integer (Theorem 1 below). If k is even, both kinds of fixable point map to just one kind—vertex or midedge according as c is even or odd respectively. If k is odd, the kinds of fixable points are preserved when c is even and exchanged when c is odd. For continuity (condition (b)), the parity of c must be the same in every tile.

These observations are summarized in a table, in which V and M denote vertices and midedges; V,M $\to x, y$ means vertices map into fixable points of kind x and midedges map into kind y.

	c even	c odd
k even	V,M $\to$ V,V	V,M $\to$ M,M
k odd	V,M $\to$ V,M	V,M $\to$ M,V

A tiling is completely characterized by its Schläfli symbol, $\{p, q\}$, which means each tile has p edges (or vertices) and each vertex is surrounded by q tiles.[6]

Planar tilings comprise {3,6}, {4,4} and {6,3} (triangles, squares and hexagons).

Spherical tilings comprise {3,3}, {3,4}, {3,5}, {4,3} and {5,3} (corresponding to the regular solids: tetrahedron, octahedron, icosahedron, cube and dodecahedron) plus the infinite classes $\{2, n\}$ (gores) and $\{n,2\}$ (hemispheres regarded as spherical polygons with n 180° angles), where n is a positive integer.[7]

In the degenerate case {2,1}, the sphere is cut by a slit that defines two coincident edges. The slit can be a great-circle arc of any positive length less than a circumference. We take a pole-to-pole slit (making one 360° gore) as a canonical representative of this uncountable subclass. Tiling projections based on {2,1} and its dual {1,2} will be discussed under the heading ''Conformal automorphisms of the sphere''.

Characterization of tiling projections

Theorem 1. In a tiling projection from spherical tiling {p,q} to planar tiling $\{p', q'\}$

(i) p *is a divisor of* p'*,*

(ii) if any spherical vertex maps onto a planar vertex, q *is a divisor of* q'*,*

(iii) if any spherical vertex maps onto a planar midedge, q *is 1 or 2, and*

(iv) if any spherical edge point maps onto a planar vertex, q' *is even.*

Proof of (i). The symmetry group of a regular n-gon is the dihedral group of order $2n$, comprising n rotations (including the identity) and n reflections. Property (i) follows from the facts that the order-$2p$ group of a spherical tile is isomorphic to a subgroup of the order-$2p'$ group of its planar image, and the order of a subgroup is a divisor of the order of a group.

The following lemma underlies the proofs of (ii)-(iv).

Lemma 1. If tile boundaries partition an arbitrarily small neighborhood of point P on the sphere, with planar image P'*, then a neighborhood of* P' *contains k images of each set in the partition, where k is a positive integer.*

Proof of Lemma 1. Let point x' in the plane trace a simple circuit around P' small enough to exclude vertices distinct from P'. For continuity, its preimage x must trace a closed (not necessarily simple) circuit C that winds around P, traversing a spherical preimage tile for each traverse of one planar tile. For C to close, C must traverse every tile incident on P the same number of times.

Proof of (ii) and (iii). When P and P' are vertices, the multiplicity in Lemma 1 is q'/q. whence property (ii). Property (iii) follows similarly from the fact that exactly 2 planar tiles touch a midedge, so q must be a divisor of 2.

Proof of (iv). The edge partitions a small neighborhood of the spherical edge point into two parts. Thus, by Lemma 1, q' must be a multiple of 2.

Corollary 1. In a tiling projection, the number, p, of vertices in a spherical tile is at most 4.

Proof. In a planar tiling, the number of vertices per tile is at most 6. Hence by Theorem 1, property (i), the number p of vertices in a spherical tile is at most 6. For $p = 6$, the only admissible Schläfli symbols—{6,2} for the sphere and {6,3} for the plane—are ruled out by property (ii), unless all 6 spherical vertices map to planar midedges. In that case spherical midedges map to planar vertices, so by property (iv) q' must be even (not

3). Hence $p < 6$.

A spherical tiling with $p = 5$ is ruled out by the lack of planar tilings in which p' is a multiple of 5.

The remaining potential pairings of spherical and planar tilings are listed in Table 1. Several of the projections lack standard names; I have taken the liberty of assigning short nicknames to all of them*. Some tiling projections can be understood in multiple ways. For example, Peirce's projection (Figure 1) can be described as a map to squares {4,4} from 2 gores (2-vertex hemispheres) {2,2}, from 4 gores {2,4}, from 4-vertex hemispheres {4,2}, or from 1-vertex hemispheres {1,2} in two ways.

Table 1. Potential and actual tiling projections. Actual projections are called by nickname and further described in Table 2. Roman numerals designate cases in Theorem 1 that prove impossibility. The starred entries generalize to five distinct one-parameter families of projections.

Spherical tiling	Planar tiling V→V		Planar tiling V→M	
	{3,6} M→M	{4,4} M→V	{3,6} M→V	{4,4} M→M
{1,2}	Hex*	Peirce*	Hex*	Peirce*
{2,1}	i	Square*	i	Adams*
{2,2}	i	Peirce	i	Peirce
{2,3}	i	ii	i	ii
{2,4}	i	Peirce	i	iii
{2,6}	i	ii	i	ii
{3,2}	Hex	i	iii	i
{3,3}	Tetra	i	iii	i
{3,4}	ii	i	ii	i
{4,2}	i	Peirce	i	Peirce
{4,3}	i	ii	i	ii

Table 2. Characteristics and origins of projections. Branch-point entries $b(e)$ give the number, b, of branch points of exponent e on the boundary of each planar tile. The measure of angles at branch points in the plane is e times the measure of corresponding angles on the sphere.

Nickname	Figure; Table	Tiles		Branch Points	Author, Date
		Spherical	Planar		
Peirce	1, 2, 11; 3(a)	hemisphere	square	$4(\frac{1}{2})$	Peirce, 1879[3]
Hex	12; 3(b)	hemisphere	triangle	$3(\frac{1}{3})$	Adams, 1925[8]
Square	13; 3(d), 4(b)	360° gore	square	$2(\frac{1}{4})$, $2(\frac{1}{2})$	Adams, 1929[9]
Adams	14; 4(c)	360° gore	square	$6(\frac{1}{2})$	Adams, 1936[10]
Tetra	15; 3(c)	tetrahedral triangle	triangle	$3(\frac{1}{2})$	Lee, 1965[11]

* Peirce and Tetra were originally called "quincuncial" and "tetrahedric".

Implementation

The first step in every construction is a standard conformal projection from sphere to plane. For all projections except Tetra, the second step is defined in terms of a standard Schwarz transform, which maps the unit disc in the z-plane onto a regular n-gon in the w-plane:

$$w = \int_0^z (1 - z^n)^{-2/n} dz \tag{2}$$

The z plane is cut from $|z| = 1$ to infinity along rays from the origin through nth roots of unity. Shifting the lower limit of the integral to $z = 1$, we obtain the alternate formula

$$w = w_n + \int_1^z (1 - z)^{-2/n} f_n(z) dz \tag{3}$$

where

$$\begin{aligned} w_n &= \int_0^1 (1 - z^n)^{-2/n} dz \\ &= \frac{1}{n} \mathrm{B}(1/n, 1 - 2/n) = \frac{\Gamma(1/n)\Gamma(1 - 2/n)}{n\,\Gamma(1 - 1/n)} \\ f_n(z) &= \left(\frac{1 - z^n}{1 - z} \right)^{-2/n} \end{aligned}$$

B and Γ are standard beta and gamma functions[12] and $f_n(z)$ is analytic and nonzero at $z = 1$. From (3) we see that the transform multiplies, by a factor of $(1 - 2/n)$, the measure of angles between lines that meet at $z = 1$. In particular, the image of a smooth curve that passes through $z = 1$ turns abruptly at $w = w_n$ making an angle of measure $(1 - 2/n)\pi$.

Tetra involves a slight variant of the preceding scheme. In Table 3(c), the rhombus $ABCE$ has angles $\pi/3$ and $2\pi/3$ in the z-plane and angles twice as large on the sphere and on its stereographic image in the w-plane. By symmetry, the short diagonal on the sphere (arc AC in stereographic projection) maps to the short diagonal in the z-plane. The exponent $-1/2$ in the integrand realizes the halving of angles.

For some wallpaper maps, the Schwarz transform is applied, as shown in Table 3, to a conformal image of the sphere stereographically projected onto the closed complex plane. For others it is applied, as shown in Table 4, to an image projected onto the unit disc by the Lagrange projection.

As inverses of doubly periodic functions, the wallpaper projections may be expressed in terms of standard elliptic integrals.[13] I have found, though, that working directly from Schwarz integrals is computationally simpler than sophisticated elliptic-integral algorithms, and just as efficient for our purpose.

Expanding the integrand in (2) by the binomial theorem yields a power series representation of the transform, with radius of convergence 1.

$$w = z \sum_{k=0}^{\infty} \binom{-2/n}{k} \frac{(-1)^k}{k + 1} z^{nk} \tag{4}$$

To evaluate the transform near the singularity at $z = 1$, change variables in (3) to place the singularity at $y = 0$.

$$\begin{aligned} w &= w_n - \int_0^{1-z} (1-(1-y)^n)^{-2/n}\, dy \\ &= w_n - \int_0^{1-z} \left(\sum_{k=1}^{n} \binom{n}{k} (-1)^{k-1} y^k \right)^{-2/n} dy \\ &= w_n - (1-z)^{1-2/n} F_n(1-z) \end{aligned} \tag{5}$$

where F_n is a power series with $F_n(0) > 0$. Table 5 gives floating-point coefficients for F_n. Using (4) in a neighborhood of $z = 0$ and (5) in a neighborhood of $z = 1$, one may evaluate the transform throughout a fundamental region, as highlighted in Tables 3 and 4. The remainder of the projection can be filled in by symmetry. I have found $|z^2| = 0.6$ to be a workable choice for the boundary between the two neighborhoods.

Similar reasoning applied to the formula for Tetra,

$$w = \int_0^z (1-z^3)^{-1/2} dz$$

leads to

$$w = \frac{\Gamma(1/3)\,\Gamma(1/2)}{3\,\Gamma(5/6)} - (1-z)^{1/2} G(1-z) \tag{6}$$

where G is a power series, coefficients for which are also given in Table 5. The series converges fast enough to be used for calculating the projection throughout the fundamental region.

Conformal automorphisms of the sphere

The fact that the center of a tile in the spherical tiling {1,2} is not fixed by its symmetry group allows wallpaper maps based on this tiling to be modified by a preparatory conformal transformation of the sphere onto itself, provided the transform respects the symmetry group. For example, if the sphere is tiled by two hemispheres with their common vertex at the north pole, a suitable preparatory transformation is to map the sphere to a polar stereographic projection at one scale and back to the sphere on another scale. Figure 2 illustrates this scheme applied to Pierce.

The transformation just described slips the equator away from the midplane of the poles, like a waistband drooping away from an ample midriff. Thus I call such a transform a *droop*. Figure 3 is an example of a globe transformed by a droop.

The same transformation idea is pertinent to a {2,1} tiling with a meridian slit of length other than π. By stereographic rescaling about the center of the tile, the length of the slit may be adjusted to π, while preserving the two reflective symmetries of the tile.

These conformal automorphisms let us generalize the starred entries in Table 1 to one-parameter families. The two starred entries for Peirce denote distinct families. In one family, the ends of the droop axis map to planar vertices; in the other (Figure 2) they map to midedges. The two starred entries for Hex, however, yield only one family. In each case one end of the droop axis passes through a vertex, the other through a midedge. The two cases differ only in regard to which end the droop is measured from. Thus the six

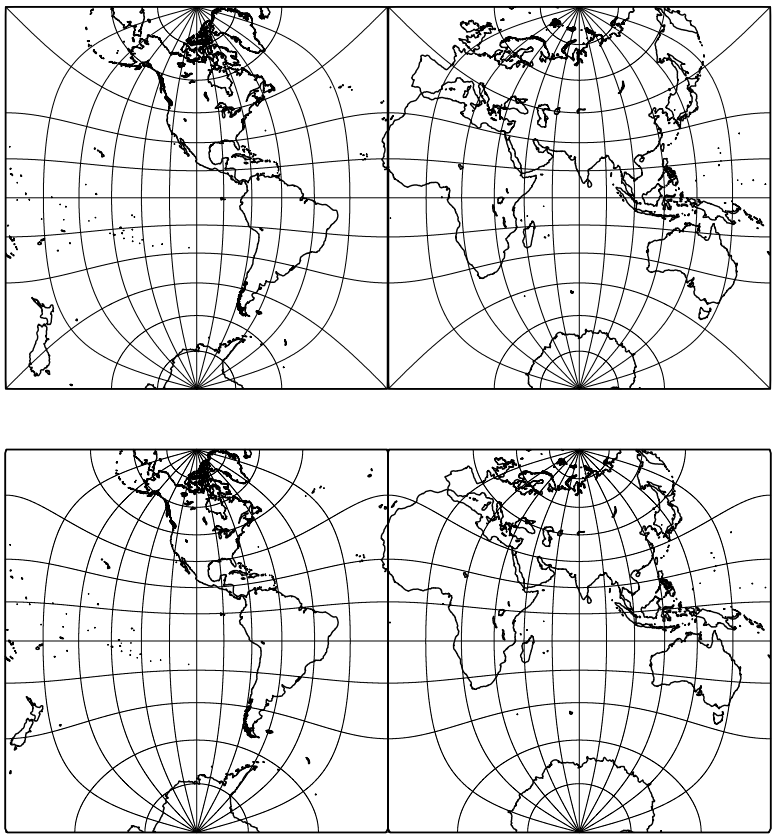

Figure 2. An aspect of the Peirce projection devised independently by Guyou.[14] At the top is a Peirce projection of two hemispheres. At the bottom, the hemispheres are regarded as {1,2} polygons with a lone vertex at the north pole. A droop shifts parallel 15°S to the normal position of the equator, emphasizing Antarctica and the Southern Ocean at the expense of the Arctic Ocean and northern Eurasia. The vertex of each hemisphere is mapped to the midedge of the edge of a square.

starred entries give rise to only five distinct parameterized families.

The choice of parameter is quite like the choice of standard parallels in more familiar projections such as the Albers or Bonne projections. In fact a convenient way to specify a polar droop is to name the parallel that becomes equidistant from the poles.

We now show that these generalizations exhaust the possibilities for wallpaper maps subject to the given symmetry conditions. The remainder of this section establishes

Theorem 2. The set of tiling projections comprises exactly the projections identified in Table 2. All but Tetra generalize to single-parameter families; Peirce generalizes in two distinct ways.

In the following discussion, the terms ‘‘meridian’’, ‘‘parallel’’, ‘‘pole’’ and ‘‘equator’’ generally refer to a mapped image of a standard spherical reticule, just as they do in discussions of a flat map, although here the image happens to lie on a sphere. Several properties of the standard reticule need not be preserved.

Meridians need not be great circles.

Parallels need not lie in parallel planes (though distinct parallels cannot intersect).

The two poles, where meridians meet, need not be antipodal.
The equator need not lie in the midplane between the poles.

Figure 3. Orthographic views from the front, side, and back of a globe transformed by a droop about (0°N, 20°E). Points on the outer edge of the front view were originally 130° away from the center.

Any conformal map of the sphere onto itself may be represented as the product of three conformal steps:

s: Map the sphere onto the closed complex plane by polar stereographic projection.
f: Conformally map the closed complex plane one-to-one onto itself.
s^{-1}: Map the plane back onto the sphere by inverse stereographic projection.

If s is taken to project a sphere of diameter 1 from viewpoint V at the south pole onto a plane tangent at the north pole (Figure 4), then spherical coordinates (θ, ϕ), where θ is measured from the north pole, map to polar coordinates (r, ϕ) and back by the formulas

$$r = s(\theta) = \tan(\theta/2), \quad \theta = s^{-1}(r) = 2\tan^{-1} r$$

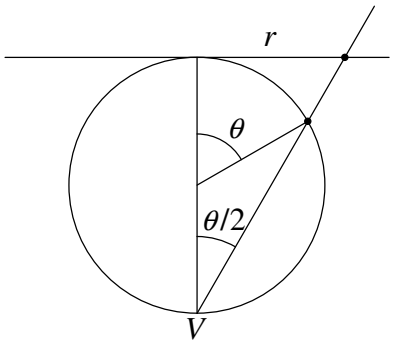

Figure 4. Construction of stereographic projection.

Function f must belong to the class of linear-fractional transforms—the only analytic functions that map the closed complex plane invertibly onto the closed complex plane.[15]

$$f(z) = \frac{az + b}{cz + d}, \quad ad - bc \neq 0$$

The four coefficients may be scaled arbitrarily. Hence three parameters suffice to identify any member of the class, from which fact follows

Corollary 2. A conformal automorphism of the sphere is determined by its behavior at three points.

Besides preserving angles, all three steps map circles onto circles.[15] (On the complex plane, straight lines count as circles of infinite radius.) Thus meridians and parallels appear on the plane as two orthogonal systems of coaxal circles,[16] illustrated in Figure 5. The meridians, which pass through the images of the north and south poles, form a coaxal system of ''intersecting type''. When the distance between poles is finite, the centers of meridians must lie on the perpendicular bisector of the segment determined by the poles. As on the sphere, parallels are trajectories orthogonal to the meridians and form a coaxal system of ''nonintersecting type''. Each parallel is disjoint from the others and separates the two poles. When the distance between poles is finite, the centers of the parallels fall on the line determined by the poles. When one pole lies at infinity, meridians become straight lines radiating from the other pole and parallels become concentric circles.

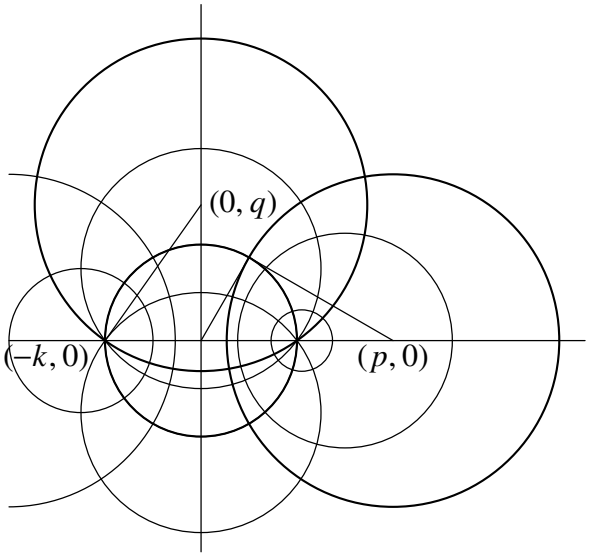

Figure 5. Representative members of two orthogonal systems of coaxal circles. Meridians are centered on the y axis and parallels on the x axis. Poles are at $(\pm k, 0)$. Meridians intersect parallels at right angles. Thick circles are a typical parallel centered at $(p, 0)$ with squared radius $p^2 - k^2$, a typical meridian centered at $(0, q)$ with squared radius $q^2 + k^2$, and the smallest meridian circle (radius k).

If s is a polar stereographic projection, and f is a dilation about the pole by a factor of m, so that the transform is a droop, the inverse stereographic projection maps parallel θ to θ' according to

$$\theta'/2 = \tan^{-1} mr = \tan^{-1}(m \tan \theta/2)$$

When $m \neq 1$, the projected parallels cluster towards one pole. The inverse of a droop with dilation factor m is a droop about the same center with dilation factor $1/m$, or equivalently a droop about an antipodal center with dilation factor m.

The conformal sphere-to-sphere transformations form an automorphism group that acts on what I call *droopy spheres.* In particular the group includes a transformation from any droopy sphere onto a *standard sphere,* where the equator lies in the midplane between antipodal poles.

Lemma 2. A droopy sphere can be transformed to a standard sphere by a single droop about an appropriate axis.

Proof of Lemma 2. If the poles of the droopy sphere are antipodal, pick any point E on the equator. There exists a droop about a pole of a standard sphere that will make the equator pass through E while preserving the poles. With the behavior of three points known, the transform is completely specified. Its inverse is the required transform.

Although we have described a droop as involving a dilation of the projection plane by some factor m, we can equally well view that as a dilation of the sphere by a factor of $1/m$. We shall do so for the rest of this section.

If the poles are not antipodal, consider first how to back-project arbitrary orthogonal systems of coaxal circles with two finite poles, N and S, and a distinguished equator onto a standard sphere. Let E be the intersection of the equator and segment NS. Figure 6 shows a cross-section of a back-projection onto a standard sphere tangent to NS. The caption explains how to determine the point of tangency, orientation, and size of the sphere.

Figure 7 shows how to arrange for three points on a droopy sphere with pole-to-equator angles of α and β to project to exactly the same three points as do the corresponding points on a standard sphere. The caption explains that, by rotating and dilating the two spheres appropriately,* their tangent points can be made to coincide. The required transformation is a droop about that point.

To complete the proof of Theorem 2, we note that a nontrivial droop preserves reflective symmetry only about planes through the axis of the droop. Hence, the axis of a droop applied to a {1,2} tiling of the sphere must pass through the single vertex through which pass the plane of symmetry for each hemispheric tile and the plane of tile-to-tile symmetry. Similarly, the axis of a droop applied to a {2,1} tiling must pass through the center of the single gore, where the gore's two planes of symmetry meet. As these are the only applicable droops, and the set of droops comprise all the nontrivial conformal automorphisms of the sphere, we have now characterized all admissible generalizations of the basic tiling projections.

Relaxed requirements

If the rather stringent conditions laid out among ''Preliminaries'' are relaxed, more wallpaper maps become possible. Some examples:

---

* Dilation and rotation parameters are calculated in Appendix 1.

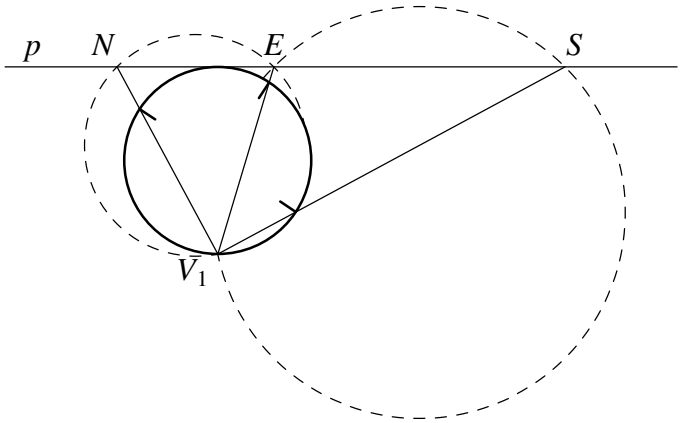

Figure 6. Back projection onto a standard sphere from an arbitrary coaxal system in plane p with poles N and S. A standard sphere, with tick marks at the poles and equator, is placed with a meridian tangent to the unique straight meridian in p. In p, the equator meets the straight meridian at E. The dashed circles are the loci of viewpoints from which NE and ES subtend $\pi/4$; V_1 is the unique viewpoint that achieves both.

1. If the projection is not required to be the same in all tiles, then the composition of any droop with any projection in Table 2 becomes admissible.
2. If a tile's symmetry group is not required to be preserved, the Cox projection[17] joins the menagerie. Cox maps a {2,1} 360°-gore tiling of the sphere onto an equilateral triangle (Table 6 and Figure 16), preserving only one of the gore's two reflective symmetries.*
3. If, further, tiles are not required to be regular polygons, then Peirce can be described in yet another way: a map from a {3,4} octahedral spherical tiling with angles $(\frac{\pi}{2}, \frac{\pi}{2}, \frac{\pi}{2})$ to a planar tiling by triangles with angles $(\frac{\pi}{2}, \frac{\pi}{4}, \frac{\pi}{4})$.

Enough. Systematic investigation of plausible generalizations is a topic for another time.

Acknowledgments

Long before I knew most of the literature cited in this paper, I showed Peirce to the late Robert Morris. He asked, ''Can you do the same thing with triangles?'' That pregnant question spurred a lasting interest in wallpaper maps.

I am grateful to Daan Strebe for pointing out references in earth-sciences literature.

Addendum

Wallpaper maps are fascinating, but are they useful? Until very recently, every instance I had seen had been published to show off the projection, not to communicate

* Adams suggested the projection in 1925, but chose not to compute it.[8] ,

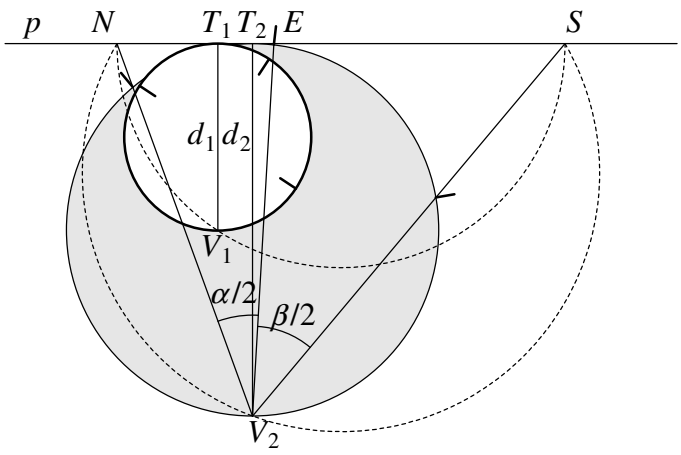

Figure 7. Mapping between a standard sphere on diameter d_1 and a gray droopy sphere on d_2. The latter sphere is oriented so that the shortest pole-to-pole meridian segment falls on the limb. Plane p, stereographic image points N, E, S and viewpoint V_1 are as in Figure 6. The dotted semicircle shows the locus of V_1 as E moves between N and S. The larger dotted arc is a typical locus of viewpoint V_2 for a droopy sphere with pole-to-equator angles α and β, where $\alpha + \beta < \pi$. The poles and equator of the droopy sphere are marked with outward-pointing ticks. As E moves monotonically from S to N, viewpoints V_1 and V_2 also move monotonically along the dotted arcs from S to N. The abscissa of V_2 lies to the left of N when E is sufficiently near N, and to the right of S when E is near S. The abscissa of V_1, however, is confined to the interval NS. By continuity, at some intermediate position of E the abscissas and associated tangent points T_1 and T_2 must coincide.

geographic information. Then, in a 2020 publication, routes of spread of Covid-19 were shown on a Peirce projection of the northern hemisphere[18] because, an author told me, it has "a nicer aesthetic than the usual polar projection." I would be pleased to hear if other uses of wallpaper maps exist.

Table 3. Construction of projections. Each left panel shows a stereographic projection in the complex z-plane. In (a), (b) and (c) the north pole is at $z = 0$ and $\arg z$ measures longitude. In (d) the north pole is at at $z = -1$ and the south is at $z = 1$. The z-plane is cut for a Schwarz transformation and scaled so cuts end on the unit circle. Similarly named labels (e.g. B, B') identify distinct approaches to the point at infinity, whose images approach a single point (B) in the w-plane. The equator is drawn with fine dashes, but only when it is circular or (piecewise) straight. Representative vertices in the w-plane are labeled by the ratio q/q', with 1/1 for a point interior to a hemispheric tile. Branch-point exponents in the Schwarz integrals are $q/q' - 1$. A shaded triangle designates a fundamental region from which the projection can be extended to the rest of the w-plane image by symmetry. (Computational formulas (4), (5) and (6) apply directly to both the fundamental region and its reflection in the real axis.)

(a) Peirce

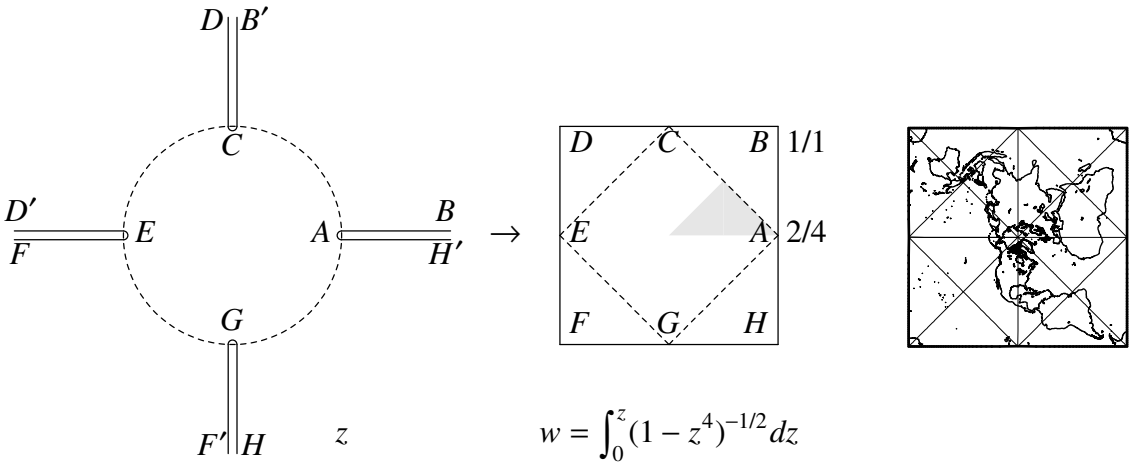

Table 3 (continued)

(b) Hex

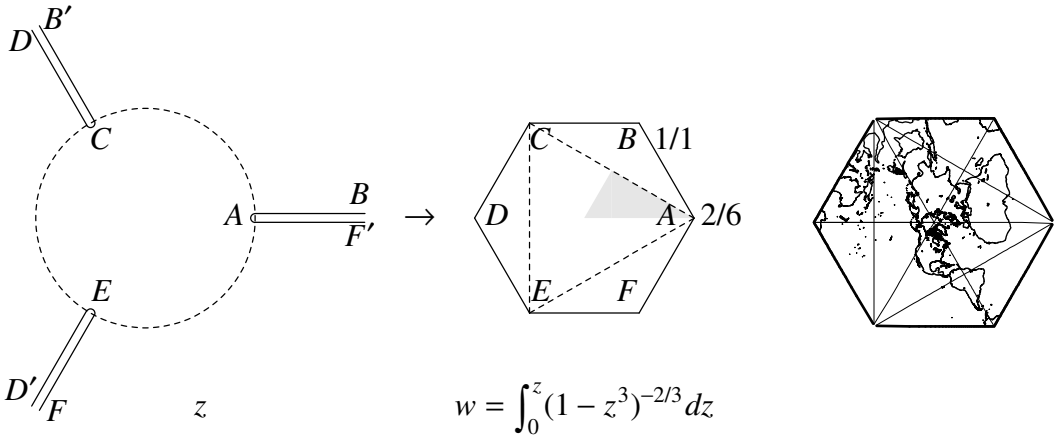

$$w = \int_0^z (1 - z^3)^{-2/3} dz$$

(c) Tetra

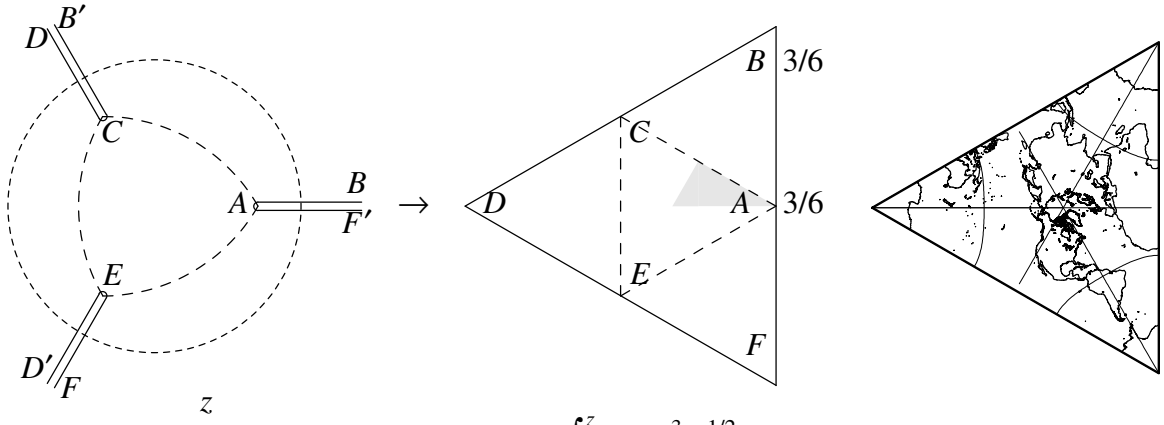

$$w = \int_0^z (1 - z^3)^{-1/2} dz$$

Spherical tile ACE has 120° angles and vertices at latitude arcsin 1/3.

(d) Square (alternate construction)

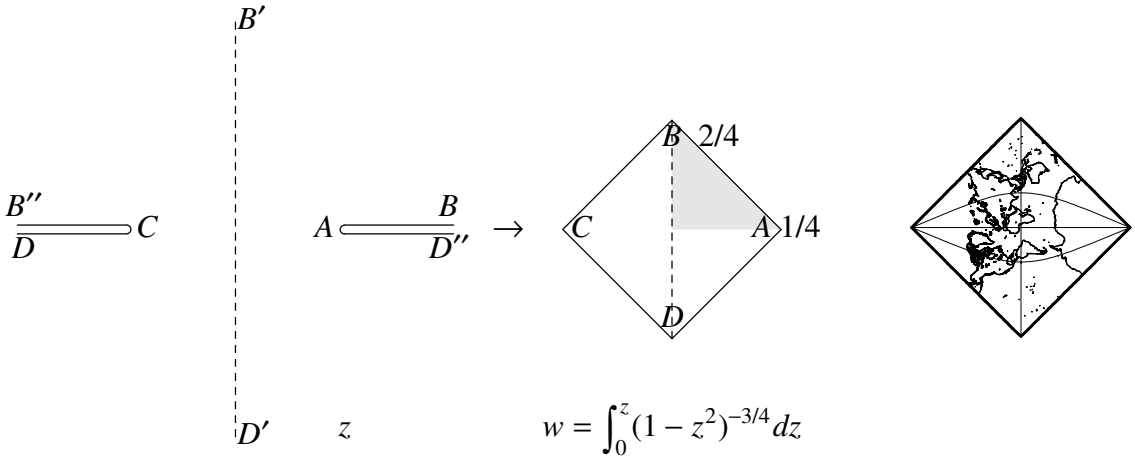

$$w = \int_0^z (1 - z^2)^{-3/4} dz$$

Fundamental region has 2 branch points; see Table 4(b) for simpler construction

Table 4. Constructions of various projections via the Lagrange projection. In the style of Table 3, (a) shows the construction of the Lagrange projection from a polar stereographic projection with the equator as unit circle. Constructions (b) and (c) start from a Lagrange projection in the complex z-plane. In (c) the z- and w-planes are rotated by $-\pi/4$ to put cuts on the axes. Every circle shown in the table is a unit circle centered at the origin.

(a) Lagrange

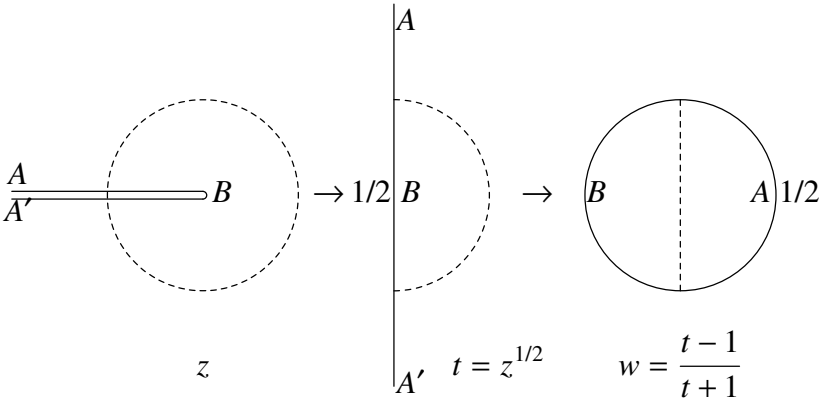

(b) Square (preferred construction)

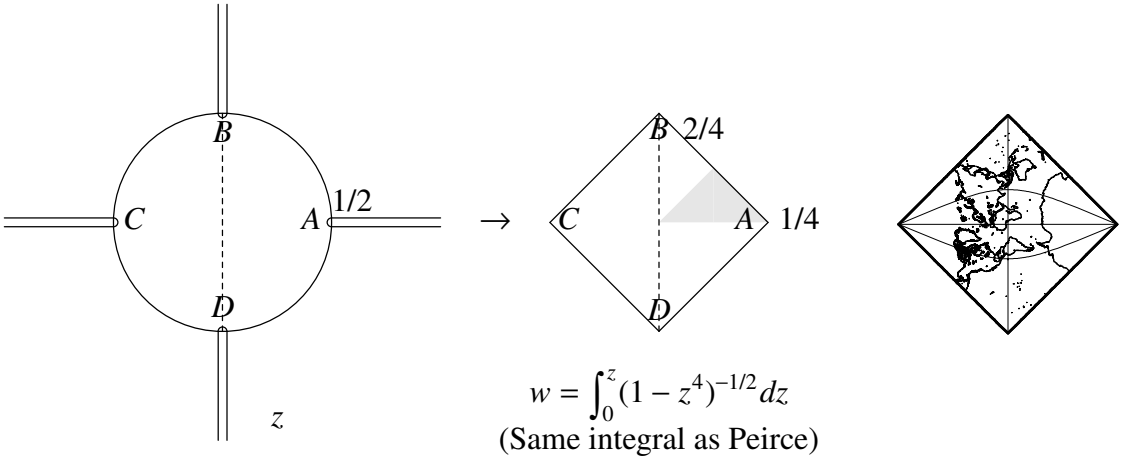

Table 4 (continued)

(c) Adams

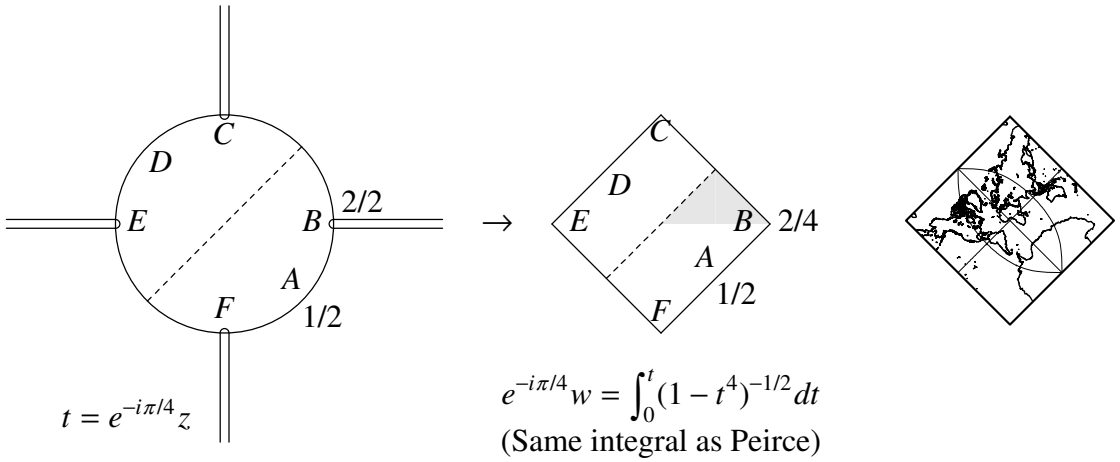

Table 5. Coefficients for power series in equations (5) and (6). A power-series package[19] was used to calculate (rational) coefficients for $n^{2/n}F_n$ and $3^{1/2}G$, from which floating-point coefficients of kth powers in F_n and G were derived. $w(1)$ is the value of w at $z = 1$ in (5) or (6).

k	F_3	F_4	G
0	1.44224957030741	1.0	1.15470053837925
1	0.240374928384568	0.25	0.192450089729875
2	0.0686785509670194	0.06875	0.0481125224324687
3	0.0178055502507087	0.0078125	0.010309826235529
4	0.00228276285265497	$-7.64973958333333\times10^{-3}$	$3.34114739114366\times10^{-4}$
5	$-1.48379585422573\times10^{-3}$	-0.0069580078125	$-1.50351632601465\times10^{-3}$
6	$-1.64287728109203\times10^{-3}$	$-2.89330115685096\times10^{-3}$	$-1.23044177962310\times10^{-3}$
7	$-1.02583417082273\times10^{-3}$	$-2.0599365234375\times10^{-5}$	$-6.75190201960282\times10^{-4}$
8	$-4.83607537673571\times10^{-4}$	$9.95881417218377\times10^{-4}$	$-2.84084537293856\times10^{-4}$
9	$-1.67030822094781\times10^{-4}$	$8.64356756210327\times10^{-4}$	$-8.21205120500051\times10^{-5}$
10	$-2.45024395166263\times10^{-5}$	$3.85705381631851\times10^{-4}$	$-1.59257630018706\times10^{-6}$
11	$2.14092375450951\times10^{-5}$	$1.40434131026268\times10^{-5}$	$1.91691805888369\times10^{-5}$
12	$2.55897270486771\times10^{-5}$	$-1.34721419308335\times10^{-4}$	$1.73095888028726\times10^{-5}$
13	$1.73086854400834\times10^{-5}$	$-1.24614486897675\times10^{-4}$	$1.03865580818367\times10^{-5}$
14	$8.72756299984649\times10^{-6}$	$-5.74855643333586\times10^{-5}$	$4.70614523937179\times10^{-6}$
15	$3.18304486798473\times10^{-6}$	$-1.12228690340999\times10^{-6}$	$1.4413500104181\times10^{-6}$
16	$4.79323894565283\times10^{-7}$	$2.27285782088416\times10^{-5}$	$1.92757960170179\times10^{-8}$
17	$-4.58968389565456\times10^{-7}$	$2.12777819566412\times10^{-5}$	$-3.82869799649063\times10^{-7}$
18	$-5.62970586787826\times10^{-7}$	$9.99206810770337\times10^{-6}$	$-3.57526015225576\times10^{-7}$
19	$-3.92135372833465\times10^{-7}$	$1.83254758167307\times10^{-7}$	$-2.2175964844211\times10^{-7}$
$w(1)$	1.76663875028545	1.31102877714606	1.40218210532546

Table 6. Constructions of the Cox projection. Construction (a) is like those of Table 3; (b) is like those of Table 4.

(a) Cox from stereographic (alternate construction)

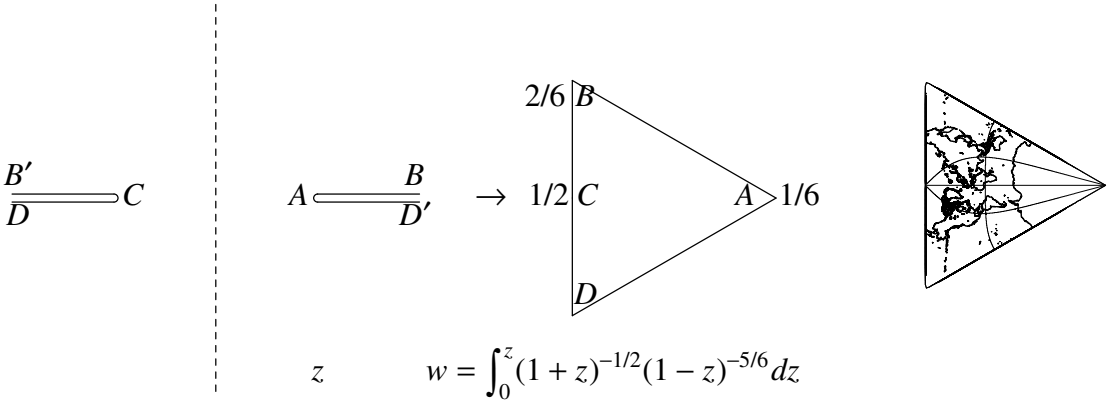

(b) Cox from Lagrange (preferred construction)

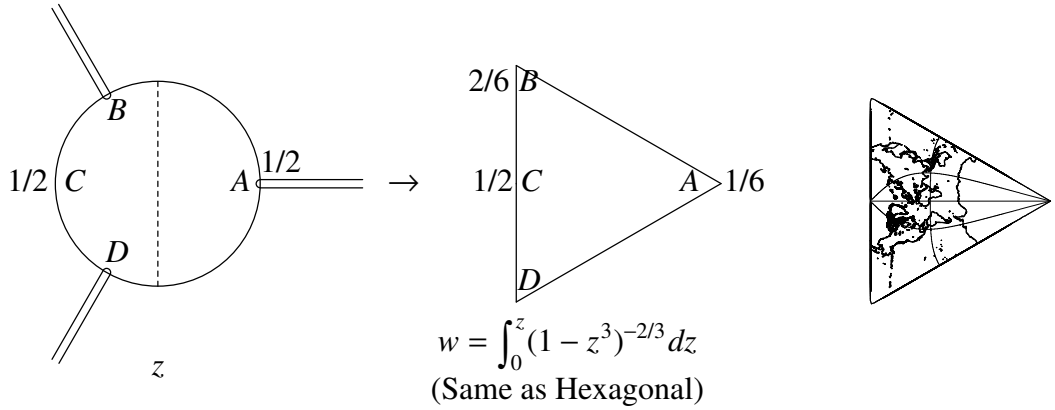

Appendix 1. Droop calculations.

Parameters of the droop that maps between a given droopy sphere and a standard sphere may be found by expressing the lengths of segments NT, ET, and ST in two ways, as projections from each sphere (Figure 8).

$$\begin{aligned} d_1 \tan\frac{\pi/2+\theta_1}{2} &= d_2 \tan\frac{\alpha+\theta_2}{2} \\ d_1 \tan\frac{\theta_1}{2} &= d_2 \tan\frac{\theta_2}{2} \\ d_1 \tan\frac{\pi/2-\theta_1}{2} &= d_2 \tan\frac{\beta-\theta_2}{2} \end{aligned} \tag{7}$$

Set $m = d_1/d_2$, $a = \tan(\frac{1}{2}\alpha)$, $b = \tan(\frac{1}{2}\beta)$, $t_1 = \tan(\frac{1}{2}\theta_1)$, $t_2 = \tan(\frac{1}{2}\theta_2)$; and use the addition formula for the tangent to obtain algebraic equations.

$$\begin{aligned} m\,\frac{1+t_1}{1-t_1} &= \frac{a+t_2}{1-at_2} \\ mt_1 &= t_2 \\ m\,\frac{1-t_1}{1+t_1} &= \frac{b-t_2}{1+bt_2} \end{aligned} \tag{8}$$

The only real solutions of (8) (found by Maple*)[20] entailed

$$m = \frac{2a^2b^2 + a^2 + b^2 \pm (4a^2b^2(1-ab)^2 + (a^2-b^2)^2\,)^{\frac{1}{2}}}{2ab(a+b)} \tag{9}$$

To choose between the two roots, consider the case $\alpha = \beta$, or equivalently $a = b$. Then, Figure 8 becomes symmetric, with T midway between N and S, and $\theta_1 = \theta_2 = 0$. Hence, from Figure 9, $m = d_1/d_2 = \tan(\frac{1}{2}\,\alpha) = a$. Specialized to $a = b$, (9) becomes

$$m = \frac{1 + a^2 \pm (\,(1-a^2)^2\,)^{\frac{1}{2}}}{2a} \tag{10}$$

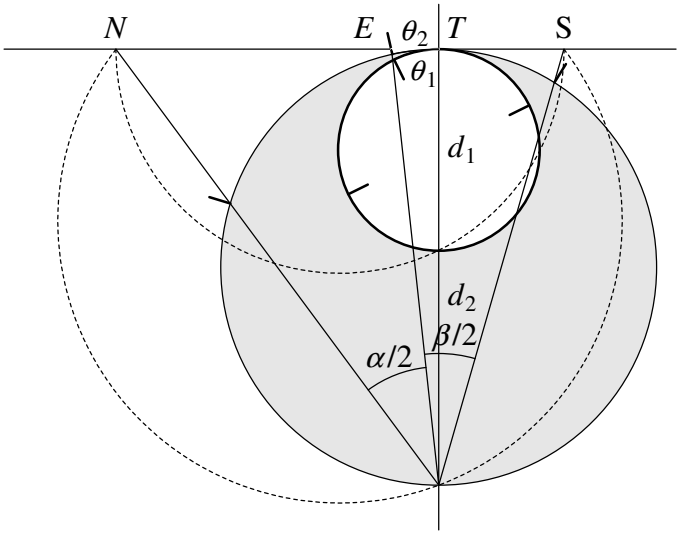

Figure 8. A standard sphere and a droopy sphere with a common point of tangency, T. θ_1 and θ_2 are azimuths of the equator measured at the center of the spheres relative to the point of tangency.

Because $\alpha + \beta < \pi$, the assumption $\alpha = \beta$ implies $a = \tan(\frac{1}{2}\,\alpha) < \tan(\frac{1}{4}\,\pi) = 1$. Thus the positive square root of $(1-a^2)^2$ is $1-a^2$. For (10) to evaluate to $m = a$, the $\pm$ sign in (9) must be taken as $-$, provided the square root is understood to be positive.

To find t_1, eliminate t_2 from (8) by simple substitution; solve each of the remaining equations for t_1^2; and equate the two results.

---

* The Maple version that I used could solve the system only after t_2 had been trivially eliminated.

$$\frac{m - a - a(m^2 - 1)t_1}{m(am - 1)} = \frac{m - b + b(m^2 - 1)t_1}{m(bm - 1)}$$

Whence

$$t_1 = \frac{a - b}{2amb - b - a}$$

Further routine manipulation leads to the complete solution of (8).

$$\begin{aligned} \frac{d_1}{d_2} = m &= \frac{2a^2b^2 + a^2 + b^2 - \sqrt{D}}{2ab(a + b)} \\ \tan\left(\tfrac{1}{2}\,\theta_1\right) = t_1 &= \frac{2a^2b^2 - 2ab + \sqrt{D}}{a^2 - b^2} \\ \tan\left(\tfrac{1}{2}\,\theta_2\right) = t_2 &= \frac{2a^2b^2 - a^2 - b^2 + \sqrt{D}}{2ab(a - b)} \end{aligned} \tag{11}$$

where

$$\begin{aligned} D &= 4a^2b^2(1 - ab)^2 + (a^2 - b^2)^2 \\ a &= \tan(\tfrac{1}{2}\,\alpha) \\ b &= \tan(\tfrac{1}{2}\,\beta) \end{aligned}$$

and $\sqrt{D}$ is understood to be positive. It may be noted that t_1 and t_2 approach 0 in the limit as b approaches a.

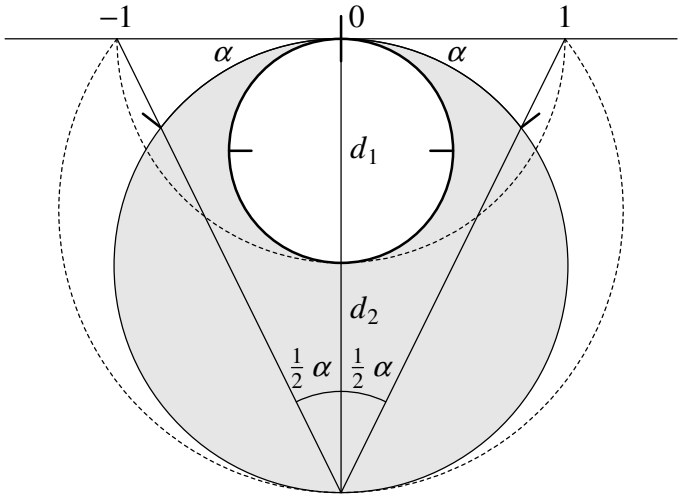

Figure 9. A droop between a standard sphere and a droopy sphere with equator midway between poles. For convenience, the distance between the projected poles is scaled to 2. Then $m = d_1/d_2 = 1/d_2 = \tan(\frac{1}{2}\,\alpha) = a$.

The shape of a droopy sphere

On a droopy sphere, meridians and parallels, being circles, lie in planes. Clearly the planes of meridians meet in the line joining the two poles. In general, the planes of parallels also meet in a common line, which must fall outside the sphere because parallels can't intersect (Figure 10).

Theorem 3. On a droopy sphere the planes of parallels concur in the line of intersection of planes tangent to the sphere at the two poles, or are parallel when the poles are antipodal.

Proof. When the poles are antipodal, the droopy sphere can be transformed to a standard sphere by a polar droop. Hence the planes of parallels must be parallel.

Otherwise, as we have seen, every droopy sphere is the inverse stereographic image of an orthogonal pair of systems of coaxal circles, with meridians meeting at two finite points. Parametric equations for such systems can be read off from Figure 5.

$$(x-p)^2 + y^2 = p^2 - k^{2,} \quad \text{parallels}$$

$$x^2 + (y-q)^2 = q^2 + k^{2,} \quad \text{meridians}$$

These equation simplify to

$$x^2 + y^2 - 2px + k^2 = 0 \tag{12}$$

$$x^2 + y^2 - 2qy - k^2 = 0 \tag{13}$$

Consider, without loss of generality, the inverse stereographic projection of systems of coaxal circles in the plane $z = 1$ (in Euclidean 3-space) onto a sphere of diameter 1 tangent to $z = 1$ at (0,0,1) with an antipodal center of perspective at (0,0,0). The equation of this sphere is

$$x^2 + y^2 + (z - 1/2)^2 = (1/2)^2$$

or

$$x^2 + y^2 + z^2 - z = 0 \tag{14}$$

To account for arbitrary positioning of the coaxal systems relative to the sphere, move the center of the coaxal systems to (a, b) by replacing x and y by $(x - a)$ and $(y - b)$ in (12) and (13). Circles of the systems are projected on sphere (14) by intersecting it with cones that have vertex (0,0,0) and coincide with the specified circles when $z = 1$.

$$(x - az)^2 + (y - bz)^2 - 2pz(x - az) + (kz)^2 = 0 \tag{15}$$

$$(x - az)^2 + (y - bz)^2 - 2qz(y - bz) - (kz)^2 = 0 \tag{16}$$

To find the intersection for a parallel, first subtract (14) from (15).

$$-2axz + a^2z^2 - 2byz + b^2z^2 - 2pxz + 2apz^2 - z^2 + z - (kz)^2 = 0$$

Factor out z to get an equation for the plane of the parallel.

$$-2(a+p)x - 2by + (a^2 + b^2 + 2ap - 1 - k^2)z + 1 = 0 \tag{17}$$

The intersection of two such planes for infinitesimally different values of p must satisfy the equation resulting from differentiating with respect to p.

$$-2x + 2az = 0 \tag{18}$$

Thus the line of intersection lies in the plane $x = az$. Substitute the value of $2x$ from (18) into (17) to find the equation of another plane in which the the line of intersection lies.

$$-2by + (b^2 - a^2 - 1 - k^2)z + 1 = 0 \tag{19}$$

Since (18) and (19) are independent of p, the line they specify is in fact the intersection of all the planes of parallels. As parallels approach the poles, their planes approach planes tangent to the sphere at the poles. Thus the common line of intersection is also the intersection of those tangent planes (Figure 10).

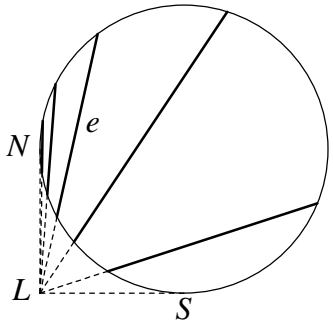

Figure 10. Cross-section of a droopy sphere, showing the planes of parallels transformed from a standard sphere with parallels spaced 30° apart. The equator is labeled e. The planes concur in line L, perpendicular to the plane of the page.

Droopy spheres have been described in the earth-science literature in connection with orthogonal grids for ocean or atmospheric circulation models.[21, 22] The cited papers suggest ‘‘rotated asymmetric bipolar grids’’ (defined by stereographic projection, linear-fractional transformation, and stereographic back-projection exactly as above) as a means for placing the singularities of a finite-difference mesh away from regions of principal interest. They do not, however, indicate that every such a grid can be created by a simple droop.

Appendix 2. Gallery.

Unit cells of the several tiling projections. The plane can be tiled continuously with translates of the figures.

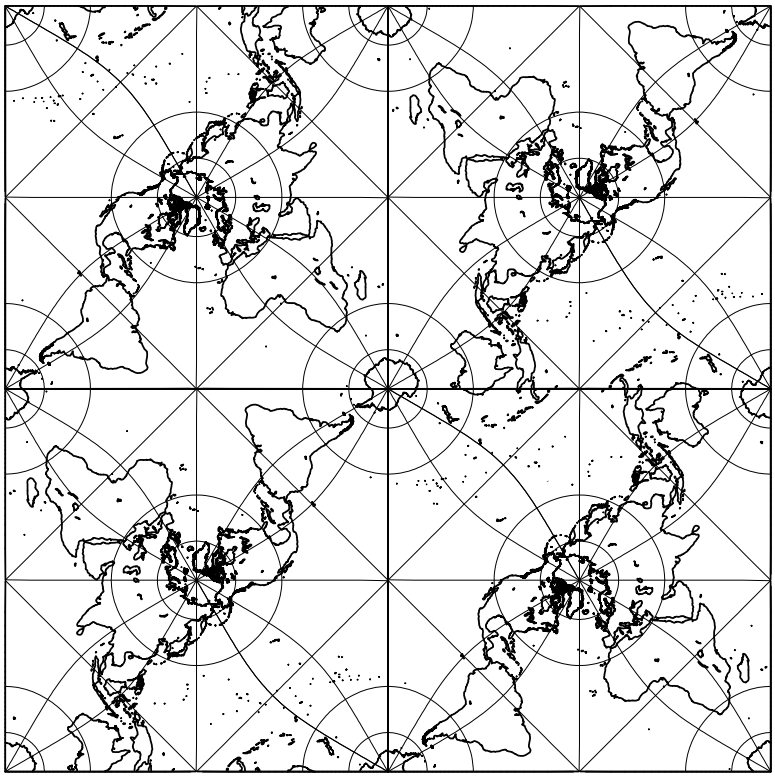

Figure 11. Unit cell for Peirce.

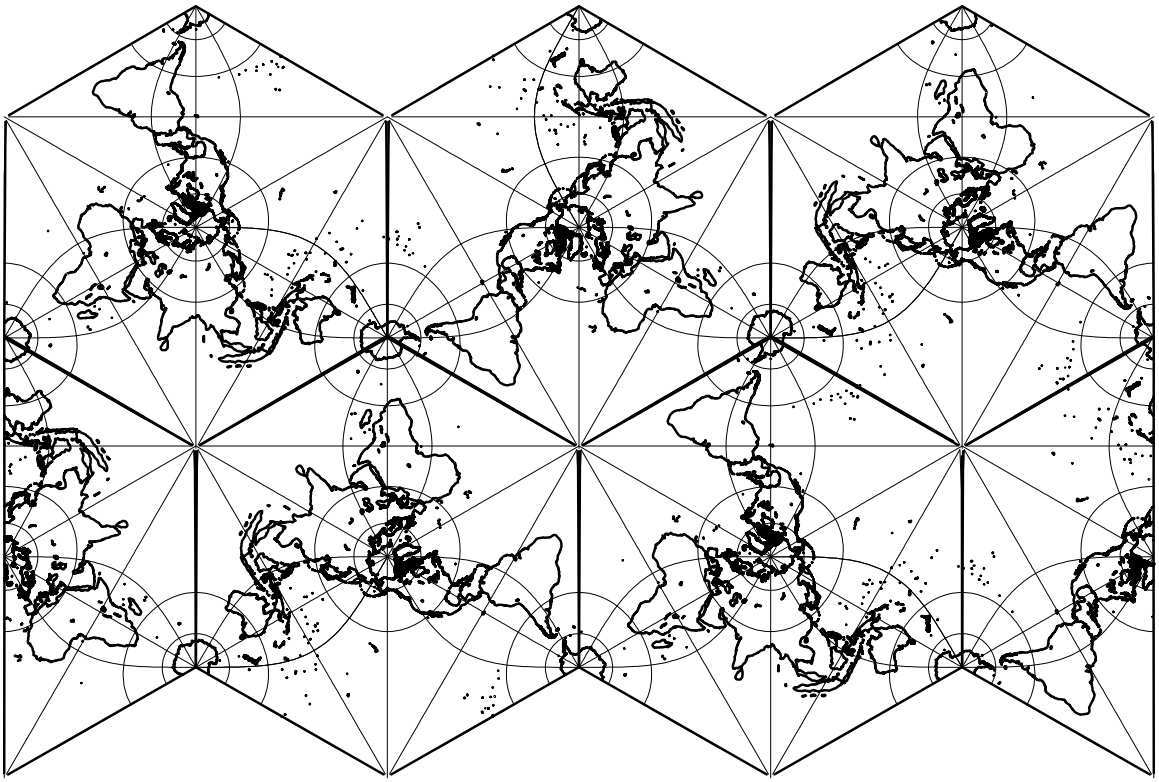

Figure 12. Unit cell for Hex.

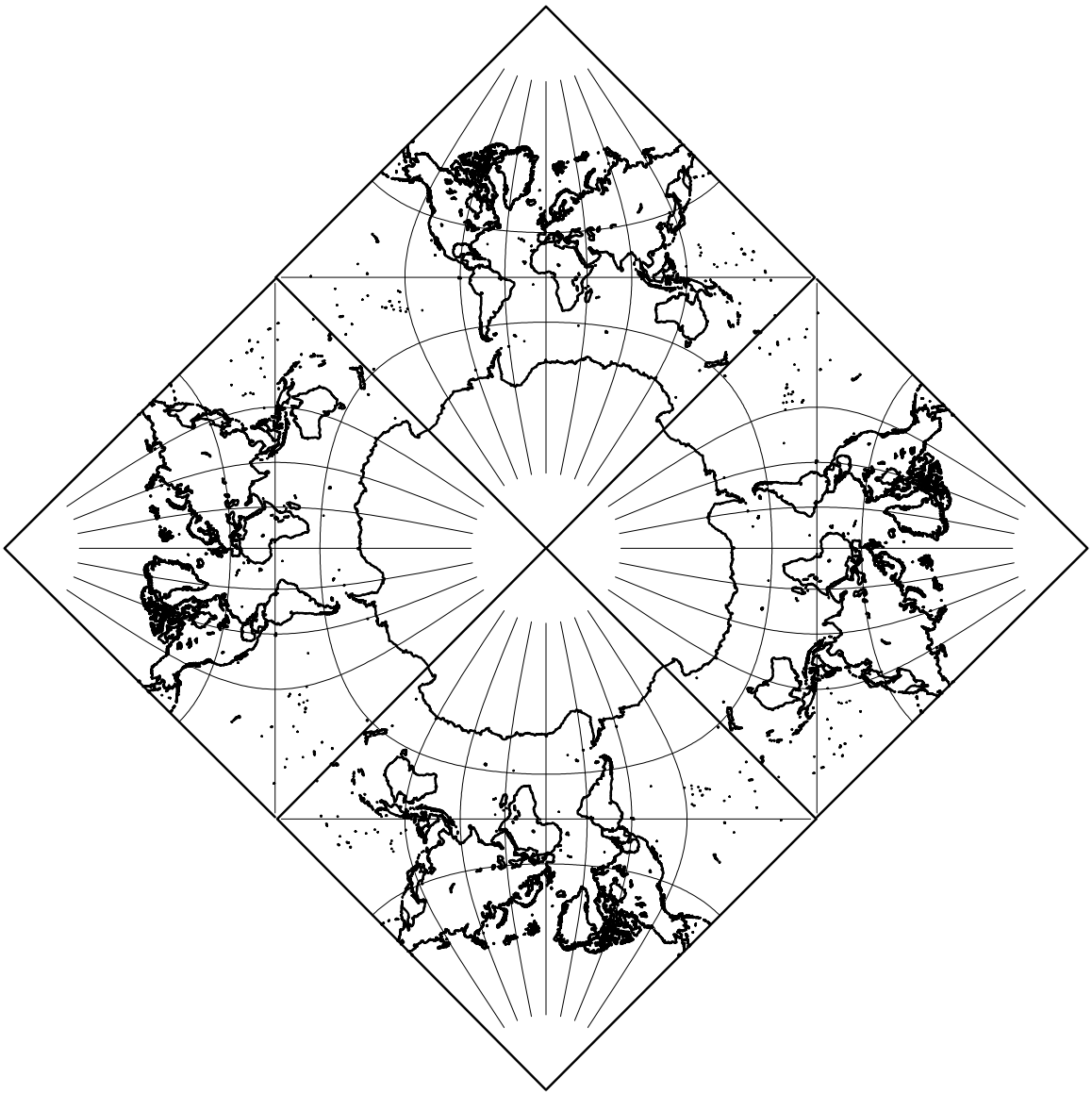

Figure 13. Unit cell for Square.

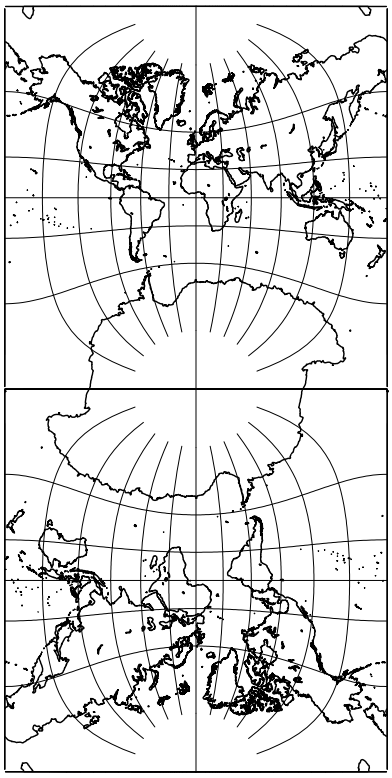

Figure 14. Unit cell for Adams.

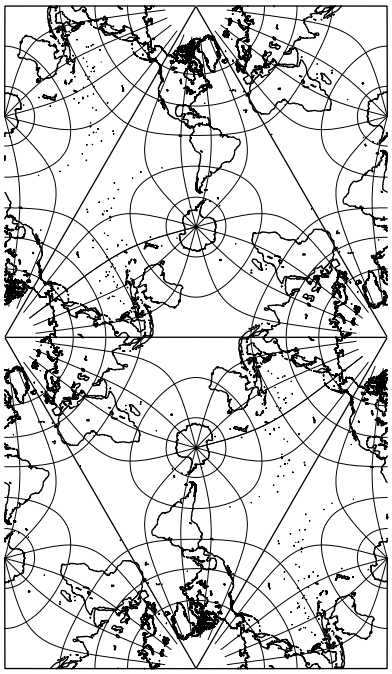

Figure 15. Unit cell for Tetra.

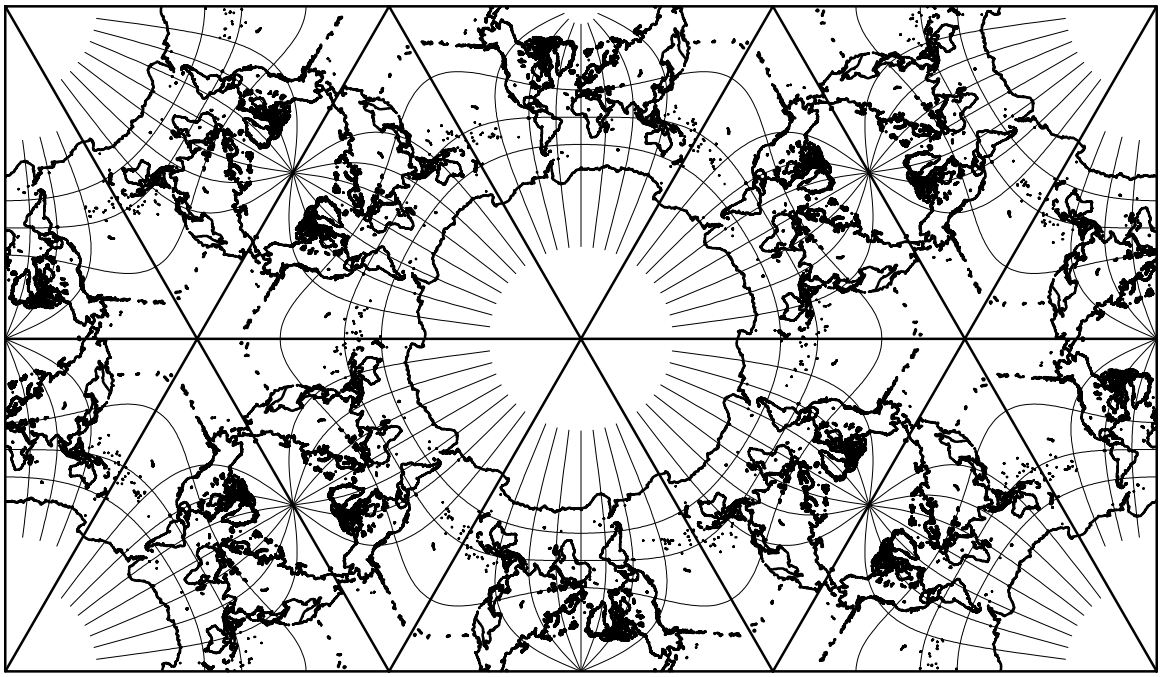

Figure 16. Unit cell for Cox. Qualifies as a tiling projection only under relaxed symmetry conditions.

References

1. M. D. McIlroy, "Wallpaper Maps," *Dependable and Historic Computing: Essays Dedicated to Brian Randell on the Occasion of His 75th Birthday,* pp. 358-375, Springer LNCS 6875 (2011), C. B. Jones and J. L. Lloyd, eds.
2. H. A. Schwarz, "Über einige Abbildungsaufgaben," *Journal für die reine un angewandte Mathematik* **70**, pp. 105-120.
3. C. S. Peirce, "A quincuncial projection of the sphere," *American Journal of Mathematics* **2**, pp. 394-396 and one unpaginated plate (1879).
4. E. T. Whittaker and G. N. Watson, *A Course of Modern Analysis,* Cambridge (1927).
5. L. P. Lee, "Conformal Projections Based on Elliptic Functions," Cartographica Monograph No. 16, University of Toronto Press (1976).
6. H. S. M. Coxeter, *Regular Polytopes,* Dover (1973). Reprint of Macmillan edition of 1963.
7. H. Weyl, *Symmetry,* Princeton University Press (1952).
8. O. A. Adams, "Elliptic Functions Applied to Conformal World Maps," Special publication No. 112, U.S. Coast and Geodetic Survey (1925).
9. O. A. Adams, "Conformal Projection of the Sphere within a Square," Special publication No. 153, U.S. Coast and Geodetic Survey (1929).
10. O. A. Adams, "Conformal map of the world in a square," *Bulletin Géodèsique,* pp. 461-473 (1936).

11. L. P. Lee, "Some conformal projections based on elliptic functions," *Geographical Review* **55**, pp. 563-580 (1965).

12. M. Abramowitz and I. A. Stegun, "Handbook of Mathematical Functions with Formulas, Graphs, and Mathematical Tables," Applied Mathematics Series no. 55, National Bureau of Standards (1965).

13. J. P. Snyder and P. M. Voxland, "An Album of Map Projections," Professional Paper 1453, U.S. Geological Survey (1989). Elliptic integrals for square tilings.

14. E. Guyou, "Sur un nouveau système de projection de la sphère," *Comptes Rendus de l'Académie des Sciences* **102**, pp. 308-10 (1886).

15. L. Bieberbach, *Conformal Mapping,* Chelsea (1953). Translated by F. Steinhardt.

16. D. Pedoe, *Geometry: A Comprehensive Course,* Dover (1988).

17. J. F. Cox, "Répresentation de la surface entière de la terre dans une triangle équilatéral," *Bulletin de la Classe des Sciences, Académie Royale de Belgique* **5^{e}, 21**, pp. 66-71 (1935).

18. M. Worobey, J. Pekar, B. B. Larsen, M. I. Nelson, V. Hill, J. B. Joy, A. Rambaut, M. A. Suchard, J. O. Wertheim, and P. Lemey, "The emergence of SARS-CoV-2 in Europe and North America," *Science* **370**, pp. 564-570 (30 Oct 2020).

19. M. D. McIlroy, "Power Series, Power Serious," *Journal of Functional Programming* **9**, pp. 325-337 (1999).

20. Waterloo Maple, Inc., *Maple User Manual,* Waterloo, ON, Canada.

21. R. J. Murray, "Explicit generation of orthogonal grids for ocean models," *Journal of Computational Physics* **126**, pp. 251-273 (1996).

22. M. Bentsen, G. Evensen, H. Drange, and A. D. Jenkins, "Coordinate transformation on a sphere using conformal mapping," *Monthly Weather Review* **127**, pp. 2733-2740, American Meteorological Society (1999).